Photo-Excited Electron and Hole Dynamics in Semiconductor Quantum Dots: Phonon-Induced Relaxation, Multiple Exciton Generation and Recombination

Kɪᴍ Hyeon-Deuk[1]

[1]*Department of Chemistry, Kyoto University, Kyoto, 606-8502, Japan*

E-mail: kim@kuchem.kyoto-u.ac.jp

Phonon-induced relaxation, multiple exciton generation and recombination (MEG and MER) govern optical properties and photo-excited dynamics in QDs. We simulated such photo-excited dynamics of electron and hole in semiconductor quantum dots (QD) by combining time-dependent *ab initio* density functional theory and non-adiabatic molecular dynamics. Our approach is based on atomictic simulations accounting for QD size, shape, defects, core-shell distribution, surface ligands, and charge trapping, which significantly influence the properties of photo-excited QDs. The calculated data were obtained as real-time photo-induced processes and described as various dynamics owing to the non-perturbative treatment of quantum transition dynamics. The simulations provide direct evidence that the high-frequency ligand modes on the QD surface play a key role in all of the electron-phonon relaxation, MEG and MER. The insights reported here suggest novel routes for controlling the photo-induced processes in semiconductor QDs and lead to new design principles for increasing efficiencies of photovoltaic devices.

KEYWORDS: quantum dot, photo-excited exciton dynamics, Auger recombination, multiple exciton generation/recombination, photovoltaic device, solar energy conversion

1. Introduction

Confinement of charge carriers in quantum dots (QDs) of sizes smaller than the Bohr exciton radius of the corresponding bulk material gives the ability to control the electronic properties by variation of QD size and shape, and leads to a variety of applications. QDs are in sharp contrast with molecular systems, whose properties vary discontinuously and require modifications in composition and structure.

Large absorption cross sections and generation of multiple electron-hole pairs make QDs excellent photovoltaic materials by providing new mechanisms for utilization of the photon energy in excess of the band gap and avoiding energy losses. Typically, significant amounts of solar power are lost to heat, limiting the maximum thermodynamic efficiency of a standard photovoltaic device to 32%. As shown in Fig.1, multiple exciton generation (MEG) creates multiple charge carriers by a single photon absorption, and provides potential for increasing photovoltaic device efficiencies. MEG yields are generally higher in QDs than in bulk [1–3], because strict conservation of translational momentum is not required in QDs due to the zero dimensionality, and the Coulomb interaction between electrons and holes, called the Auger interaction, is enhanced due to closer proximity of charge carriers. On the contrary, multiple exciton recombination (MER), in combination with electron-phonon relaxation, reduces photovoltaic efficiencies by accelerating energy losses to heat. MEs convert to single excitons (SEs) of higher energy that is ultimately dissipated by phonons.

Recent experiments reported the enhanced photon-to-charge conversion due to the MEG in PbSe QD-based solar cells, as manifested by increased photo-current. [4, 5] At the same time, the diverse and conflicting reports on MEG efficiencies show that the dynamics and mechanisms of MEG and MER are still poorly understood and remain controversial. In particular, surface-induced charge trapping and related processes are believed to be the source of the discrepancies in the MER and MEG signals and their interpretation. Our real-time atomistic simulation method gives a novel and comprehensive perspective on dynamics of photo-excited charge carriers in nanoscale materials and provide important insights into the mechanisms and efficiency of MEG and MER.

2.   Method : time-dependent *ab initio* theory for MEG and MER

We developed the theoretical methods which enable the current time-domain *ab initio* simulation to study photo-excited dynamics in semiconductor nano materials. Our state-of-the-art simulation combines time-domain density functional theory (TDDFT) with non-adiabatic molecular dynamics (NAMD). [6–9] The electronic structure and adiabatic MD were computed with VASP using a converged plane-wave basis in a cubic simulation cell periodically replicated in three dimensions. Spurious interactions of periodic images were prevented by including at least 8 Å of vacuum between QD replicas. The PW91 density functional and projector-augmented-wave pseudopotentials were used to preserve computational efficiency, which is particularly important for our real-time TDDFT simulations that include explicit couplings to phonon modes. The initial QD geometry was generated from bulk, passivated by hydrogen atoms as needed, fully optimized at zero temperature, and heated up to ambient temperatures by MD with repeated nuclear kinetic energy rescaling. Microcanonical trajectories of 5 ps to 30 ps were produced using the Verlet algorithm with a 1 fs time-step and the Hellman-Feynman force in the ground electronic state.

The Auger dynamics involving SE and double exciton (DE) states coupled to nuclear motions were simulated using TDDFT formulated in the adiabatic KS basis. [6–8] In the adiabatic representation, all Coulomb interactions appearing in the electronic Hamiltonian are "diagonalized out" during the calculation of the adiabatic states, and transitions between different SE and DE states occur due to the NA coupling. The atomistic simulation of the SE/DE generation and recombination dynamics was performed with fluctuating NA couplings and energies calculated by VASP. Our method differs from other approaches such as the conventional Fermi's golden rule by simultaneously taking into account the MEG, MER, and phonon-assisted processes in a real-time atomistic simulation. The atomistic simulation allows us to study the roles of surface ligands, dopants, defects, unsaturated chemical bonds, size, shape, and other realistic properties of QDs in the MEG and MER dynamics. The NA coupling terms are calculated non-perturbatively in our simulation, leading to non-exponential MEG and MER dynamics. This bypasses the limitations of Fermi's golden rule that adopts perturbative treatment and implicitly assumes exponential decay. Additionally, the present explicit time-domain simulations account for phonon dynamics, including high-frequency surface ligand modes. These properties are typically omitted in static rate theories.

3.   Results : real-time MEG and MER dynamics

We demonstrated the importance of the ligand contribution to the Auger processes based on our time-domain simulation studies. We investigated the Auger-type MEG and MER dynamics in small Si QDs of different size and with different surface passivation, and compared the Si results with those for a CdSe QD. [7] Our earlier study focused on a Ge QD. [6]

3.1 Static properties of representative QDs

The SE and DE DOS of the three small QDs, (A) Si_{10}, (B) Cd_6Se_6, and (C) $Si_{29}H_{24}$, are shown in Fig.2. The underlying atomic structure, thermal fluctuations, as well as the Coulomb interactions break the electronic degeneracy, creating a complicated multilevel band structure and a distribution of energies for each state. Note that our time-domain simulation used band structure calculated for each instantaneous geometry along the trajectory and thus discrete energy levels. The three QDs allow us to investigate simultaneously the effects of material type, size, ligands, and excitation energy on the efficiency and mechanisms of the MEG and MER processes. The surface of the larger Si QD is passivated by hydrogens that eliminate unsaturated chemical bonds more efficiently than surface reconstruction alone. As a result, the HOMO-LUMO energy gap of the hydrogen-passivated Si QD is very close to the gaps of the smaller and bare Si and CdSe QDs; 2.0 eV, 2.0 eV, and 2.1 eV for Si_{10}, Cd_6Se_6, and $Si_{29}H_{24}$, respectively even though the gap is generally inversely proportional to the QD diameter. The DOS is clearly larger in $Si_{29}H_{24}$ than in the smaller QDs, as seen in the y-axis scales of the different panels. The DE DOS starts at twice higher energy than the SE DOS, but the former rapidly becomes dominant due to the increasing combinatorial number of DEs with energy. The ratio of the DE DOS to the SE DOS is largest for $Si_{29}H_{24}$ at high energies. The analysis of the SE and DE DOS suggests that excited state population will shift to DEs at high energies and to SEs at low energies.

The geometric and electronic structures of the QDs are illustrated in the inserts of Fig.2. The left-most panels present geometry snapshots from the dynamics simulation at ambient temperature. All QDs preserve the original bulk topology at room temperature, bonds do not break, and defect states do not appear within the gap. The middle and right panels of the inserts display the HOMO and LUMO charge densities, respectively. The orbitals of the smaller cluster appear notably more localized, compared to the $Si_{29}H_{24}$ QD where the HOMO and LUMO are delocalized over the core region due to the more homogeneous bonding pattern. The hydrogen ligands passivating the $Si_{29}H_{29}$ surface affect the orbitals; the LUMO is delocalized over the hydrogen ligands more substantially than the HOMO.

3.2 Real-time MEG with phonon couplings

The decay of the total population of all SEs shown in Fig.2 indicates that MEs appear starting from an initially excited SE of high energy. Our simulation includes SEs, DEs, and the ground state, but the ground state population remains negligible throughout several picoseconds of the NAMD simulation, in agreement with the experiments [10–12]. The MEG dynamics studied here strongly depends on the initial excitation energy as reported in the experiments. The energy dependence of the MEG rates arises mainly from the rapid increase of the DE DOS with energy. The MEG dynamics is faster in Si_{10} than Cd_6Se_6, as indicated by the lines (A) and (B). This is because the ratio of the DE DOS over the SE DOS is larger in the former than in the latter QD.

Most other theories focus on MEG rates by assuming an exponential MEG process. The MEG dynamics in the smaller QDs are well fitted by the Gaussian functions, indicating that the DE DOS that couple to the SE states is relatively small, and that a rate description, such as Fermi's golden rule requiring a high density of final states, is not applicable there. On the other hand, the MEG data for the large QD can be fitted by a combination of Gaussian and exponential functions because sufficiently many DEs participate in the MEG dynamics at a later time.

Our NAMD study explicitly includes phonon dynamics, and therefore allows for phonon-assisted Auger processes. Indeed, we demonstrated the phonon-assisted MEG starting at energies lower than $2E_g$. The high frequency Si-H phonon modes in the $Si_{29}H_{24}$ QD enabled this phonon-assisted MEG: the electronic degrees of freedom can borrow energy from high energy phonons and allow the MEG even below the purely electronic threshold.

3.3 Phonon mode analysis for MEG and MER

In order to characterize the phonon modes that couple SE and DE states, we computed the Fourier transforms of the corresponding, time-dependent energy gaps. The electronic energies fluctuate due to coupling to phonons, and the energy gap fluctuation is directly related to the electron-phonon coupling. The spectra for the three QDs are presented in the right panels of Fig.2. The Si_{10} phonons are higher in frequency than the Cd_6Se_6 phonons, accelerating the faster MEG dynamics in the Si_{10} QD. The light hydrogen atoms passivating the surface of the $Si_{29}H_{24}$ QD introduce additional high frequency modes up to 2000 cm^{-1}, increasing the efficiency of phonon-assisted MEG. The ligand contribution to the QD electronic states and electron-phonon coupling should decrease with increasing QD size due to the reduced surface-to-volume ratio.

3.4 Efficient MER

Our simulation involves simultaneously a variety of processes, enabling us to study the interplay between MEG and MER, and to provide additional physical details of the combined MEG/MER dynamics. Figure 3 shows the SE population dynamics accompanying the DE generation. The data are plotted as a 2D function of time and energy. The initial SE evolves into other SEs, and at around 1 ps, the total SE population becomes small as a result of the MEG, in harmony with the accelerating MEG at around 1 ps in Fig.2. The SE population starts to reappear at a lower energy after 1.5 ps-2 ps. This population recursion directly reflects the MER, demonstrating that our approach simultaneously takes into account both the MEG and MER. The MER time of 1.5 ps-2 ps agrees with the experimental results for small QDs. [13–16] In comparison, MER starting from a single DE state takes several hundred picoseconds. [7] A superposition of many DEs produced by the preceding MEG process enables multiple coupling pathways to a broader range of SEs, producing the reasonable MER timescale estimate. In other words, the MEG is more efficient than the diffusion from the initially excited single DE. This effect is particularly pronounced for the MER compared to the MEG, since the density of final SE states in the MER is much lower than the density of final DE states in the MEG, and it is important to couple to as many final states as possible in order to achieve the efficient MER.

4. Concluding Remarks

In summary, we developed and performed the time-domain, atomistic, *ab initio* studies of photo-excited carrier relaxation, MEG and MER dynamics in semiconductor QDs of different size and material, with and without ligands. Since these photo-excited dynamic processes dominate excitation and charge dynamics in most nanoscale systems, the developed approach can find many applications in the future. Our atomistic method is very well suited to investigate defects, ligands, charges, dopants and dangling bonds, which could play extremely important roles in excitation dynamics of QDs. Actually, our studies provided the first direct evidence that the phonon modes of the passivated QD surfaces play a vital function in the photo-excited carrier dynamics in semiconductor QDs. By selecting a ligand, one should be able to control and manipulate, to a large extent, charge carrier relaxation in semiconductor QDs. Carefully controlled synthetic inorganic chemistry involving reactions between inorganic semiconductors and molecular ligands is a very valuable tool needed for advancing experimental aspects of QD research aimed at efficient harvesting and conversion of solar energy.
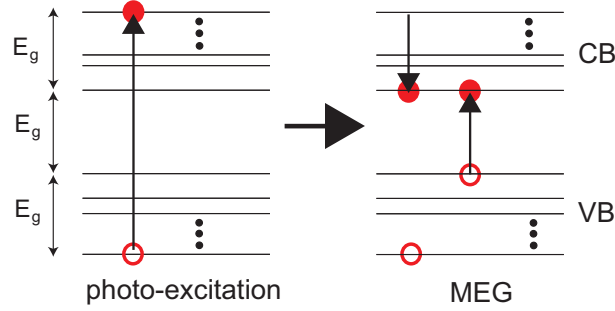
**Fig. 1.** Schematic mechanism of the MEG.
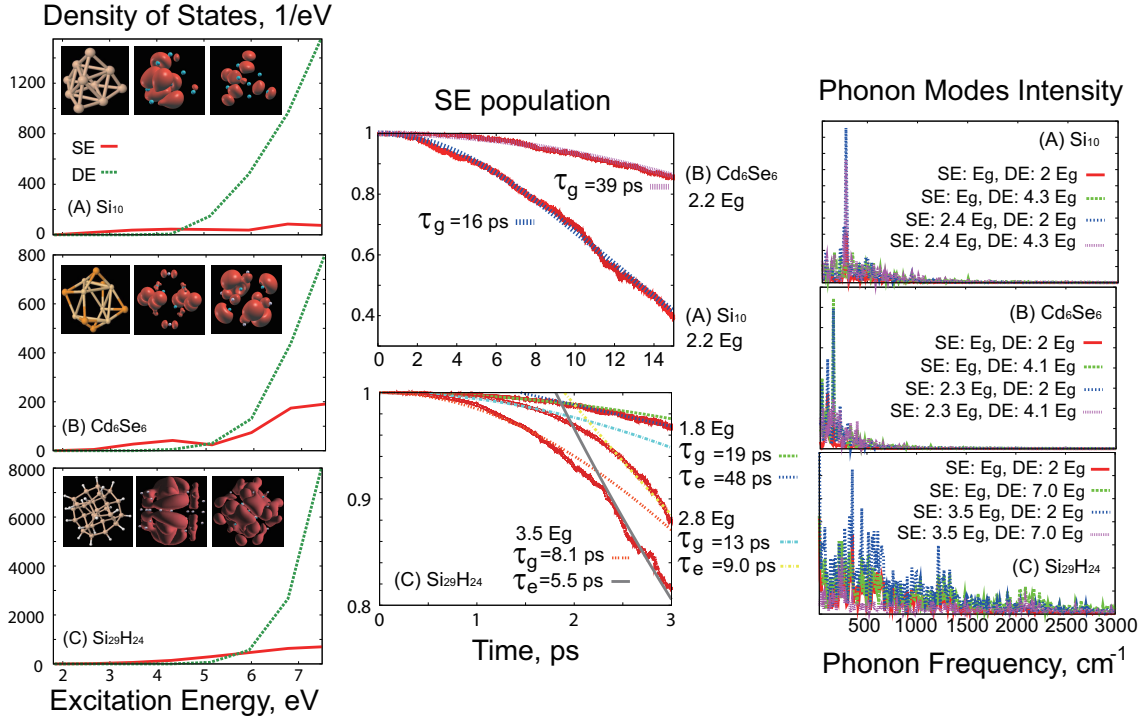
Fig. 2. (Left panels) SE and DE DOS of (A) Si_{10}, (B) Cd_6Se_6, and (C) $Si_{29}H_{24}$. The DE DOS starts at higher energies than the SE DOS, but the former rapidly overtakes the latter as the energy increases. The DOS is much higher in $Si_{29}H_{24}$ than in the smaller QDs, and the DE/SE DOS ratio increases most rapidly. Typical structures from a dynamics trajectory at the ambient temperature, and charge densities of the HOMO and LUMO states are shown from left to right in each panel. (Middle panels) Total population of all SEs starting from an initially excited SE of the displayed energy. The population decrease due to the MEG. The MEG follows Gaussian decay in the smaller clusters, while the MEG in $Si_{29}H_{24}$ exhibits a transition from the Gaussian to the exponential decay. The slow phonon-assisted MEG is observed at energies below $2E_g$ in $Si_{29}H_{24}$. The Gaussian and exponential timescales, τ_g and τ_e, are displayed. The MEG is faster in Si_{10} than in Cd_6Se_6, reflecting the larger DE/SE ratio in Si_{10} around 2.2 E_g. (Right panels) Phonon modes that couple the SE and DE pairs displayed in each panel. The phonon peaks appear at higher energies in lighter Si_{10} than in heavier Cd_6Se_6, supporting the faster MEG in Si_{10}. $Si_{29}H_{24}$ exhibits a broader phonon spectrum, and possesses high-frequency Si-H phonon modes, leading to the efficient phonon-assisted MEG.
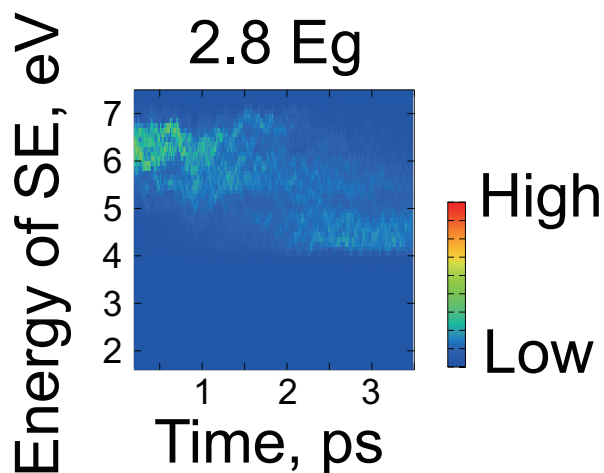
Fig. 3. SE population dynamics in $Si_{29}H_{24}$ as a two-dimensional function of time and SE energy. The initially excited SE evolves into other SE states. The decrease in the SE population seen at intermediate times corresponds to the MEG shown in Fig.2. The recursion of the SE population at a later time corresponds to the MER, demonstrating that our method accounts for MEG and MER simultaneously. The obtained MER timescale of 1 ps to 3 ps agrees with the experimental observations for small QDs [13–16].

References

[1] J. A. McGuire, J. Joo, J. M. Pietryga, R. D. Schaller and V. I. Klimov *Acc. Chem. Res.* **41** (2008) 1810.

[2] A. J. Nozik *Chem. Phys. Lett.* **457** (2008) 3.

[3] M. C. Beard, A. G. Midgett, M. C. Hanna, J. M. Luther, B. K. Hughes and A. J. Nozik *Nano Lett.* **10** (2010) 3019.

[4] O. E. Semonin, J. M. Luther, S. Choi, H.-Y. Chen, J. Gao, A. J. Nozik and M. C. Beard *Science* **334** (2011) 1530.

[5] J. B. Sambur, T. Novet and B. A. Parkinson *Science* **330** (2010) 63.

[6] K. Hyeon-Deuk and O. V. Prezhdo *Nano Lett.* **11** (2011) 1845.

[7] K. Hyeon-Deuk and O. V. Prezhdo *ACS Nano* **6** (2012) 1239.

[8] K. Hyeon-Deuk and O. V. Prezhdo J. Phys.: Cond. Matt. **24** (2012) 363201.

[9] K. Hyeon-Deuk and O. V. Prezhdo *Dalton Trans.* **45** (2009) 10069.

[10] J. J. Peterson and T. D. Krauss *Nano Lett.* **6** (2006) 510.

[11] M. Nirmal, B. O. Dabbousi, M. G. Bawendi, J. J. Macklin, J. K. Trautman, T. D. Harris and L. E. Brus *Nature* **383** (1996) 802.

[12] M. Sykora, L. Mangolini, R. D. Schaller, U. Kortshagen, D. Jurbergs and V. I. Klimov *Phys. Rev. Lett.* **100** (2008) 067401.

[13] R. D. Schaller, J. M. Pietryga and V. I. Klimov *Nano Lett.* **7** (2007) 3469.

[14] I. Robel, R. Gresback, U. Kortshagen, R. D. Schaller and V. I. Klimov *Phys. Rev. Lett.* **102** (2009) 177404.

[15] Y. Kobayashi, L. Pan and N. Tamai *J. Phys. Chem. C* **113** (2009) 11783.

[16] Y. Kobayashi, T. Nishimura, H. Yamaguchi and N. Tamai *J. Phys. Chem. Lett.* **2** (2011) 1051.